PCCP

Cite this: *Phys. Chem. Chem. Phys.*, 2011, **13**, 17756–17767

www.rsc.org/pccp

PAPER

Electric field-controlled dissociation and association of porphyrin J-aggregates in aqueous solution

Kazuaki Nakata,[a] Takayoshi Kobayashi[bcde] and Eiji Tokunaga*[af]

Received 16th June 2011, Accepted 15th August 2011
DOI: 10.1039/c1cp21964b

The electrooptic effects of porphyrin J-aggregates of tetraphenyl porphyrin tetrasulfonic acid (TPPS) in aqueous solution were studied using electroabsorption (EA) spectroscopy. When the J-aggregates were three-dimensionally distributed, the EA spectra exhibited broadening in the exciton band. When a DC or AC electric field was applied for a long time, the J-aggregates with KCl were dissociated into monomers *via* *N*-mers (N = 2–4) as intermediate states, while those without KCl had an increase in aggregation. The EA spectra showed a red shift in the exciton band for *N*-mers, which indicates that *N*-mers are isolated microaggregates with a coherent aggregation number N, and isolated microaggregates have not been microscopically or spectrally observed until now. The estimated third-order nonlinear optical susceptibility $\chi^{(3)}$ for EA spectra in aqueous solution was 10^4 times larger than that in a polymer film. The molecular rearrangement model was applied to a variety of orientational distributions and the results were explained fairly well. The contribution of the electric double layer is the most probable reason for the large enhancement of $\chi^{(3)}$ for the solution sample. The dynamic equilibrium between two types of monomers, J-aggregates of various aggregation numbers and cations such as K^+ and H^+ was investigated to reveal that K^+ is more loosely bound to the constituent monomers in J-aggregates than H^+. Equilibrium equations also show that well-grown aggregates with $N > 15$ tend to dominate in a solution of J-aggregates, which explains why only well-developed aggregates can be observed spectroscopically.

Introduction

In recent years, self-assembled organic and inorganic nanowires and nanotubes have received much attention due to their potential application as functional nanomaterials. Among them, self-assembled molecular J-aggregates are prominent candidates for nanoscale optoelectronic devices, because J-aggregates have a sharp absorption band and a large transition dipole moment with large optical nonlinearity due to Frenkel exciton formation.[1–12]

There is experimental evidence[13–18] that J-aggregates have a hierarchical structure. Those observed as rod-like shapes by near-field optical microscopy,[14–16] electron microscopy,[17] and atomic force microscopy (AFM)[18] are macroaggregates, which are composed of an incoherent ensemble of the microaggregates. The latter is a one-dimensional assembly of monomer molecules, whose arrangement determines the interaction energy, J, between the transition dipole and neighboring transition dipole. An image of microaggregates has never been obtained in microscopic experiments. Coherent extension of the Frenkel exciton defines the coherent aggregates, the size of which is the same as that of the microaggregates. Spectroscopic investigation is important to provide information on the coherent aggregates; however, presently observed spectra are inhomogeneously broadened due to the formation of macroaggregates.

There are two forms of the monomer in an aqueous solution of tetraphenyl porphyrin tetrasulfonic acid (TPPS). One of the two forms is an F-monomer, or free-base monomer, which is a tetravalent anion (H_2TPPS^{4-}) with D_{2h} symmetry. The other is a D-monomer, which is a diacid and is a divalent anion (H_4TPPS^{2-}) with D_{4h} symmetry. The D-monomer is formed when two protons are inserted in the central cavity of the porphyrin ring of the F-monomer. This is realized, for

[a] *Department of Physics, Faculty of Science, Tokyo University of Science, 1-3 Kagurazaka, Shinjuku-ku, Tokyo 162-8601, Japan. E-mail: eiji@rs.tus.ac.jp*
[b] *Advanced Ultrafast Laser Research Center, and Department of Engineering Science, Faculty of Informatics and Engineering, University of Electro-Communications, 1-5-1, Chofugaoka, Chofu, Tokyo 182-8585, Japan*
[c] *Institute of Laser Engineering, Osaka University, 2-6 Yamada-oka, Suita, Osaka 565-0871, Japan*
[d] *Core Research for Evolutional Science and Technology (CREST), Japan Science and Technology Agency, 4-1-8 Honcho, Kawaguchi, Saitama 332-0012, Japan*
[e] *Department of Electrophysics, National Chiao Tung University, 1001 Ta Hsueh Rd., Hsinchu 30010, Taiwan*
[f] *Research Center for Green and Safety Sciences, Tokyo University of Science, 1-3 Kagurazaka, Shinjuku-ku, Tokyo 162-8601, Japan*

example, in a low pH solution. Both monomer molecules have two absorption bands, which are referred to as the B band (or Soret band) in the near UV to blue range and the Q band in the visible region.

The monomer that constitutes the J-aggregates is considered to have the D monomer structure, because the positively charged center of one H_4TPPS^{2-} molecule attracts the negatively charged peripheral substituents of adjacent molecules to form a linear assembly with slipped face-to-face stacking.[19] The monomer has two orthogonal transition dipole moments in the molecular plane, so that the assembly simultaneously forms J- and H-aggregates. Between these two forms, the optical properties of the D-monomer are less characterized, because it tends to be assembled to form macro J-aggregates in solution and micro J-aggregates are difficult to observe in a polymer matrix. J-aggregates have strong optical anisotropy; the dipole moment of the J band is parallel to the J-aggregates orientation axis, the *J*-axis, and that of the H band is perpendicular to the *J*-axis.

Electroabsorption (EA) or Stark spectroscopy is an established method to analyze the properties of electronic transitions. It can be used to determine the differences in the polarizability and transition dipole moment between the ground and excited states with the symmetry properties of the transition, and third-order nonlinear optical susceptibility.[20] It can also be used to detect charge transfer states and optically forbidden states. Stark spectroscopy has provided results regarding molecular aggregates,[21–23] and photosynthesis proteins and pigments.[24–29] EA spectroscopy has been mainly applied to solid samples such as crystals and pigments embedded in polymer matrices.[21–29] Solution samples have been studied only in exceptional cases, most of which have been restricted to organic solvents.[30–32] EA spectroscopy of polar molecules in aqueous solution has never been reported to the best of our knowledge. The unique properties of electrooptic response in J-aggregates are expected to emerge in aqueous solution, because they are self-assembled in aqueous solution.

We have previously reported the results of EA spectroscopy of J-aggregates composed of TPPS in a polymer film.[1–3] When the J-aggregates are distributed two-dimensionally in a polymer film, the difference in the static polarizability, $\Delta\alpha$, between the excited and ground states, is almost 100 times larger for the J-aggregate than for the monomer.[1,2] In addition, the $\Delta\alpha$ of the J-band exhibited signal strength saturation with application of a strong electric field, and the magnitude of the EA spectrum signal was reduced to less than 1/10 by lowering the temperature from room temperature to 77 K.[3] It is difficult to explain these results in terms of a purely electronic response. Instead, we proposed a molecular rearrangement model to explain the giant electrooptic effects of TPPS J-aggregates in the films.[2,3] The model was further supported by the results for aqueous solution and a quasi-one dimensionally oriented film.[3] We concluded that molecular rearrangement is the main mechanism of the giant electrooptic response in TPPS J-aggregates.[3]

In the present work, we report a more comprehensive and detailed study on the electrooptic response of TPPS J-aggregates in aqueous solution than that provided in ref. 3, where electroabsorption spectroscopy of J-aggregates in aqueous solution was introduced for the first time. EA spectra of the aqueous solution have provided signals 10 000 times larger than that for a polymer film, and control of the number of aggregated molecules was found to be possible using an external electric field.

Experimental

Two types of solution samples were used in the present study. One solution, without KCl, was prepared by dissolving specific amounts of TPPS (4 mg, 0.8 mmol l^{-1}) in 5 mL of water. Fig. 1a shows the absorption spectrum of this solution. There are two absorption peaks; the J band due to the Frenkel exciton located at 490 nm, and the monomer band attributed to the D-monomers exhibited by the broad peak at 433–435 nm. This indicates that the solution contains both aggregates and monomers. The other solution with KCl was prepared by the addition of TPPS (3.6 mg, 0.77 mmol l^{-1}) and KCl (39 mg, 0.1 mol l^{-1}) in 5 mL of water. Two absorption peaks, the J- and H-bands (423 nm), were observed for this solution and are shown in Fig. 1c. Therefore, this indicates that the solution contains only J- and H-aggregates.

The solution was placed in a gap of 0.07 mm between a pair of transparent electrodes composed of the indium tin oxide (ITO) film on a glass plate. The thickness of the ITO layer, the resistivity, and carrier density were 300 nm, 1.3×10^{-4} Ω cm, and 1.2×10^{21} cm^{-3}, respectively. A 0.07 mm thick plastic film with a 12×12 mm^2 hole for containment of the solution was sandwiched as a spacer between the ITO glass plates ($25 \times 25 \times 1$ mm^3).[33,34]

EA or electromodulation (EM) spectra were phase-sensitively detected using a multi-channel lock-in amplifier combined with a polychromator.[35] The non-polarized white light from a Xe lamp (Hamamatsu, L2273) was collimated after being focused through a 0.2 mm pinhole and then loosely focused to an area of 10 mm diameter on the sample. A modulated external electric field of $F = F_0 \sin 2\pi ft$ with $F_0 = 8.6 \times 10^3$ to 7.1×10^2 V m^{-1} at $f = 221$ Hz was applied between the electrodes using a function generator (NF, 1956 multifunction synthesizer) for both samples, with and without KCl.

The absorbance changes detected at modulation frequency f and its second harmonic $2f$ are due to the Pockels and Kerr effects, respectively. Here, we have focused on the Kerr response, for which $\Delta\alpha$ was deduced from the red shift of the B band (Soret band) of the J-aggregates. The method of data analysis followed is given in ref. 1, 19 and 35. The change in absorption can be written as

$$\Delta A = A_0 \frac{dA}{dE} \Delta\mu s F + \frac{1}{2} B_0 \frac{dA}{dE} \Delta\alpha (sF)^2 + \frac{1}{2} C_0 \frac{d^2A}{dE^2} |\Delta\mu|^2 (sF)^2, \quad (1)$$

where F is the applied electric field, s is a local field factor, and A_0, B_0, and C_0 are fitting parameters relevant to the degree of molecular orientation. Eqn (1) indicates that the difference in the polarizability ($\Delta\alpha$) and in the static dipole moment ($\Delta\mu$) between the excited and ground states can be evaluated by fitting the change in absorbance with the first and second derivatives of the absorption spectrum, respectively. There is some uncertainty in the values for constants such as

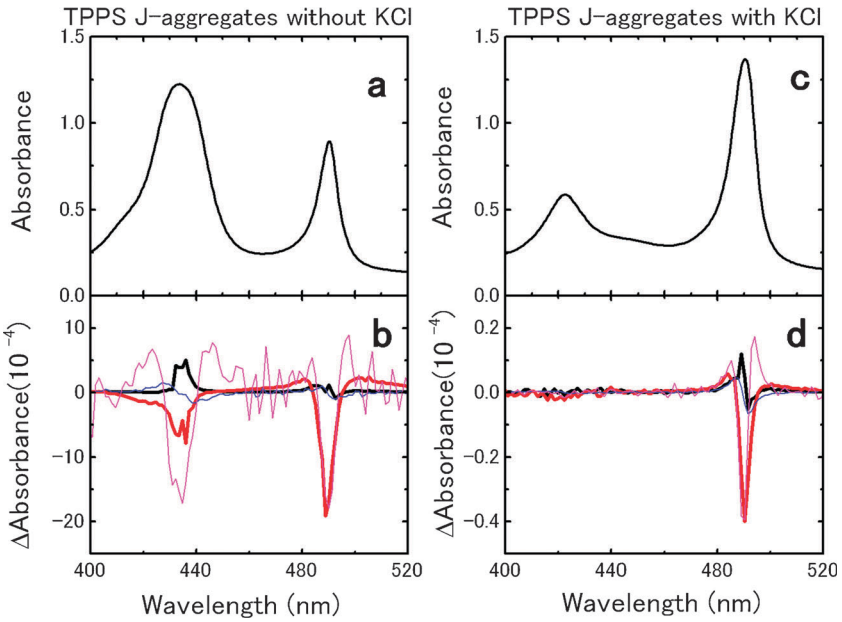

Fig. 1 Absorption and electroabsorption (EA) spectra of TPPS J-aggregates in aqueous solution without (a, b) and with (c, d) KCl. The concentration of TPPS for (a, b) is 8×10^{-4} mol l^{-1}. The concentrations of TPPS and KCl for (c, d) are 7.7×10^{-4} mol l^{-1} and 0.1 mol l^{-1}. Black, red, blue, and magenta lines are X-phase spectra, Y-phase spectra, fitting curves to Y, and fitting curves to X for EA spectra, respectively. The applied electric fields were $F_0 = 8.6 \times 10^3$ V m^{-1} (b, without KCl) and $= 7.1 \times 10^2$ V m^{-1} (d, with KCl). The reference frequency was 221 Hz.

B_0 and s; therefore, these are defined in the electrooptical parameters used in the present study, as follows:

$$s^2 Tr(\Delta\alpha) B_0 = C_1 \frac{hc}{F_0^2} \frac{10^{40}}{1.113} \quad (2)$$

$$s|\Delta\mu| C_0^{\frac{1}{2}} = C_2^{\frac{1}{2}} \frac{hc}{F_0} \frac{10^{30}}{3.34}, \quad (3)$$

where h is the Planck constant, c is the speed of light, and C_1 and C_2 are fitting constants from the first and second derivatives of the absorbance, respectively.

The component of $\Delta\alpha$ (tensor) was previously[1,2] compared between the J-aggregate and the monomer by assuming that the J-aggregate and monomer have one-dimensional and two-dimensional structures, respectively. In contrast, we follow the convention to use $Tr\Delta\alpha$ for the difference in the static polarizability, because it is questionable as to whether the macro-aggregate can be regarded as one-dimensional. Note that the enhancement factor in $Tr\Delta\alpha$ by the aggregate formation in a polyvinyl alcohol (PVA) film is not almost 100 times, as reported in ref. 1, but is approximately 50 times.

An irreversible change in the absorption spectra was induced by a stationary electric field for a period of about 1 h. This is referred to as the long-time response of the absorption spectra to a constant electric field. An electric field with $F_0 = 2.9 \times 10^4$ V m^{-1} (DC) or 3.4×10^4 V m^{-1} (AC) was applied between the electrodes using the function generator. Spectra were obtained every minute by scanning the wavelength repetitively with a spectrophotometer (Shimadzu, UV-3150). In addition, during the time course of the irreversible change under the AC electric field, EA spectra or electromodulation (EM) spectra were successively measured every 7 min. The prompt acquisition of EA spectra was facilitated with the use of the multichannel lock-in detection method. In order to discriminate the EA spectra from the electric-field induced irreversible change in the absorption spectra, EM spectra were often used instead of EA spectra.

Results

Fig. 1b and d show EA spectra of TPPS J-aggregates in aqueous solution, with and without KCl, respectively. Both spectra were fit reasonably well by the second derivative of the absorption spectra, showing broadening in the absorption bands.

Fig. 2 shows the long-time response of the absorption spectra with DC (Fig. 2a and b) and AC (Fig. 2c) electric fields over 60 and 120 min, respectively. In the case of the solution without KCl (Fig. 2a), the absorption strength of the J band increased, while that of the D-monomer band decreased with time. In contrast, for the solution with KCl (Fig. 2b and c) the peak energy, intensity, and spectral bandwidth of the J-band blue-shifted, decreased, and increased, respectively. At the same time, the F-monomer band peak at 412–413 nm increased on the shorter wavelength side of the H band, while that of the H band decreased, as shown in Fig. 2b. The spectra in Fig. 2c under an AC electric field showed gradually a blue-shift of the J-band accompanied by an increase of the F-monomer peak. The peak energy represented by N, which corresponds to N-mers, continuously varied from $N > 16$ to $N = 4$ (tetramers), $N = 3$ (trimers), and $N = 2$ (dimers) as intermediate states, and finally to that of the F-monomer. The coherent aggregation number N was estimated using eqn (4). When the dissociation made substantial progress, the J band no longer recovered within 2 h after the electric field was turned off, which implies that dissociation occurred irreversibly. In addition, the blue shift of the F-monomer band was observed when the electric field was applied for more than 2 h.

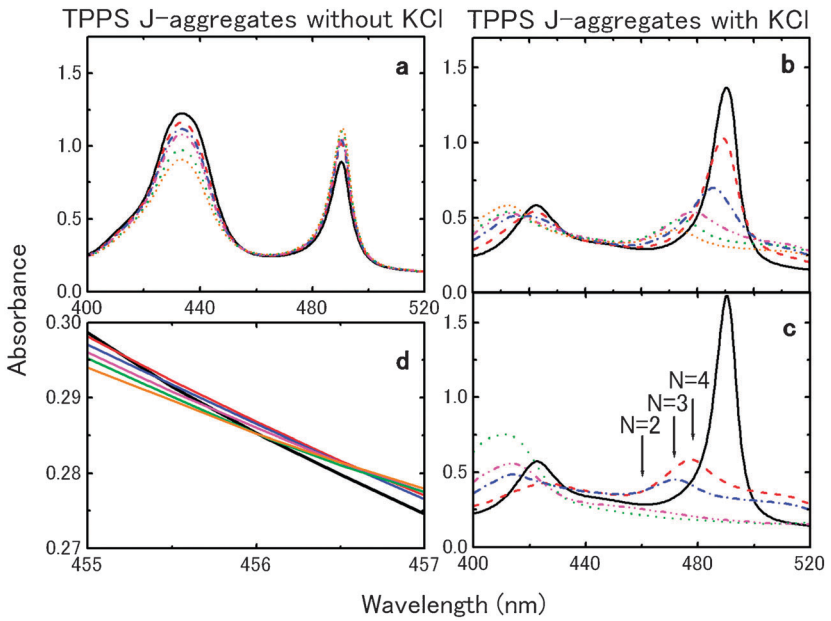

Fig. 2 The long-time response of absorption spectra measured with application of (a, b) DC and (c) AC electric fields for 1 and 2 h, respectively. The concentration of TPPS for (a, d) is 8×10^{-4} mol l^{-1}. The concentrations of TPPS and KCl for (b, c) are 7.7×10^{-4} mol l^{-1} and 0.1 mol l^{-1}. Without KCl, the respective increase and decrease in the height of the J-band and the D-monomer band was observed (a). The spectra from 455 to 457 nm are magnified in (d) to show the isosbestic point. With KCl, the dissociation of J-aggregates was observed under the electric field (b, c). For (a and b), black (solid), red (dashed), blue (dash-dotted), magenta (dash-dot-dotted), green (dotted), and orange (short dashed) lines are the absorption spectra at 0, 10, 15, 20, 40, and 60 minutes after the time when the DC electric field was applied, respectively, with $F = 2.9 \times 10^4$ V m^{-1}. In (c), absorption spectra of TPPS J-aggregates ($N \gg 10$), TPPS tetramers ($N = 4$), trimers ($N = 3$), dimers ($N = 2$), and F-monomers are represented by black, red, blue, magenta and green, lines, respectively, with $F_0 = 1.7 \times 10^4$ V m^{-1}. The reference frequency was 221 Hz.

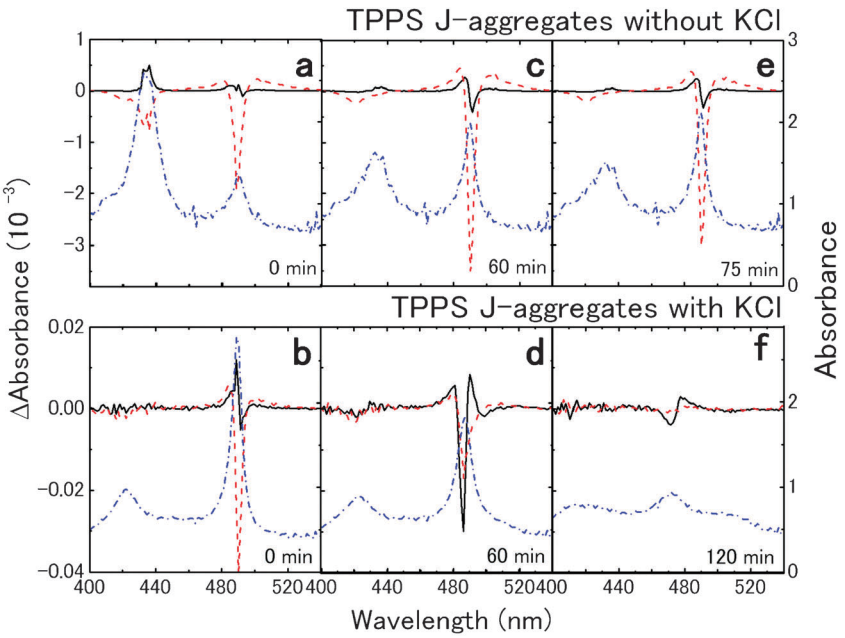

Fig. 3 Long-time response of EA and absorption spectra of TPPS J-aggregates without (a, c, e) and with KCl (b, d, f) measured under the electric field for 2 hours. The concentration of TPPS for (a, c, e) is 8×10^{-4} mol l^{-1}. The concentrations of TPPS and KCl for (b, d, f) are 7.7×10^{-4} mol l^{-1} and 0.1 mol l^{-1}. For samples with KCl, aggregation numbers of the coherent TPPS J-aggregates N in b, d and f are >10, ~ 10 and <10, respectively. Black (solid), red (dashed) and blue (dash-dotted) lines are EA spectra of X-phase, those of Y-phase and absorption spectra, respectively. The spectra measured at 0, 60, 75, and 120 minutes after the time when the electric field was applied are shown in (a, b), (c, d), e, and f, respectively. The electric fields were $F_0 = 8.6 \times 10^3$ V m^{-1} (a, c, e) and $= 7.1 \times 10^2$ V m^{-1} (b, d, f), respectively.

Table 1 Electrooptic parameters of TPPS J-aggregates for isotropic distribution in aqueous solutions and for the two-dimensionally distributed film in ref. 1. $\chi^{(3)}$ in the first and second line is estimated from the $Tr\Delta\alpha$ and $\Delta\mu$, respectively. $\chi^{(3)}$ due to the broadening signal for the aqueous solution is formally evaluated from $\Delta\mu$, but is physically originated from $\Delta\alpha$ as discussed in the text

	$s^2Tr\Delta\alpha B_0$ (Å^3)	$s\Delta\mu C_0{}^{0.5}$ (D)	$\lvert\chi^{(3)}\rvert$ (esu)	$\lvert\chi^{(3)}\rvert$ (esu/molecule)
With KCl, $N > 10$	-4×10^8		1.1×10^{-3}	3.3×10^{-19}
		50	1.9×10^{-5}	5.7×10^{-21}
With KCl, $N \approx 10$	1.4×10^9		2.8×10^{-3}	8.3×10^{-19}
		35	9.3×10^{-6}	2.8×10^{-21}
With KCl, $N < 10$	6×10^9		4×10^{-3}	1.2×10^{-18}
Without KCl	$1.2–1.9 \times 10^8$		$0.8–3.2 \times 10^{-4}$	9.5×10^{-20}
		600–1000	$6.5–9.7 \times 10^{-6}$	2.8×10^{-21}
PVA film	~15000	~0.1	7.6×10^{-10}	5.4×10^{-25}

Table 2 Electrooptic parameters with the local-electric factor s equal to $(\varepsilon + 2)/3$ in the Lorentz field, where ε is the dielectric constant; $\varepsilon_{H_2O} = 80$ and $\varepsilon_{PVA} = 5.9$

	$Tr\Delta\alpha B_0$ (Å^3)	$\Delta\mu C_0{}^{0.5}$ (D)	$\lvert\chi^{(3)}\rvert$ (esu)	$\lvert\chi^{(3)}\rvert$ (esu/molecule)
With KCl, $N > 10$	-5.4×10^5		1.1×10^{-6}	3.3×10^{-22}
		1.9	1.9×10^{-8}	5.7×10^{-24}
With KCl, $N \approx 10$	1.9×10^5		2.8×10^{-6}	8.3×10^{-22}
		1.3	9.3×10^{-9}	2.8×10^{-24}
With KCl, $N < 10$	8.2×10^6		4×10^{-6}	1.2×10^{-21}
Without KCl	$1.6–2.6 \times 10^5$		$0.8–3.2 \times 10^{-7}$	9.5×10^{-23}
		22–37	$6.5–9.7 \times 10^{-9}$	2.8×10^{-24}
PVA film	~2000		7.6×10^{-11}	5.4×10^{-26}

Fig. 3 shows the successive change in the EA spectra during the time course of the change in the absorption spectra under constant electric field for solutions without (Fig. 3a, c and e) and with KCl (Fig. 3b, d and f). The absorption and EA spectra are shown at $t = 0$ (Fig. 3a and b), 60 (Fig. 3c and d), 75 (Fig. 3e), and 120 (Fig. 3f) min after the onset of the electric field. The absorption spectra were calculated from the multi-lock-in signals using $A = -\log(T_t/T_0)$, where T_0 is the intensity of the probe light without the sample and T_t is that with the sample at the corresponding time. There was no substantial change in the EA signal for the solution without KCl, while a characteristic change was observed for the solution with KCl; the initial broadening signal changed to a red-shifted signal as the absorption peak blue-shifted with time.

Table 1 lists the estimated electrooptic parameters, $\Delta\alpha$, $\Delta\mu$ and the third-order nonlinear optical susceptibility $\chi^{(3)}$ [36] for isotropic distribution of the TPPS J-aggregates in aqueous solution and for the two-dimensionally distributed film given in ref. 1. $\chi^{(3)}$ per molecule for the solution is 10^4 times larger than that for the polymer film. Note that the magnitude of $\Delta\alpha$ is larger with than without KCl. The broadening signal typically reflects the difference in the static dipole moment $\Delta\mu$; however, in the rearrangement model, it is explained by the change in the polarizability difference, $\Delta\alpha$.[3]

Table 2 lists the same data with explicit consideration for the Lorentz local-field factor s, which is expressed by $(\varepsilon + 2)/3$, where ε is the dielectric constant with $\varepsilon_{H_2O} = 80$ and $\varepsilon_{PVA} = 5.9$. After this correction, $\chi^{(3)}$ per molecule for the solution is 10^2 times larger than that for the polymer film. We use the concentration of the TPPS in the polymer film as 2×10^{19} molecules in the estimation.

Discussion

Molecular rearrangement model

For J-aggregates, the excitation energy is dependent on the aggregation number and the molecular arrangement of the constituent monomers as:

$$E_k = E_0 + 2J\cos\left(\frac{k\pi}{N+1}\right) = E_0 + 2\frac{M^2}{4\pi\varepsilon_B r^3}(1 - 3\cos^2\theta)\cos\left(\frac{k\pi}{N+1}\right), \quad (4)$$

where E_0 is the excitation energy of monomer molecules, M is the transition dipole moment between the relevant electronic states in the molecule, r is the intermolecular distance, ε_B is the background permittivity, θ is the angle between the molecular transition dipole moment and the intermolecular bonding axis connecting the centers of the transition dipoles, *i.e.* *J*-axis, and N is the aggregation number forming the coherent (micro)aggregate.[2,37]

The molecular rearrangement model, which was introduced in ref. 2, can explain the energy shift of TPPS J-aggregates by the change in J, *i.e.*, the interaction energy between monomer transition dipoles induced by the applied field. In this model, the observed energy shift for 2-dimensional distributions in ref. 1 and 2 is reproduced by a change in θ, as small as $\Delta\theta = 0.002°$. The relative direction of the *J*-axis in the model with respect to the electric field vector $\boldsymbol{F}$ influences the change in the excitation energy of J-aggregates.

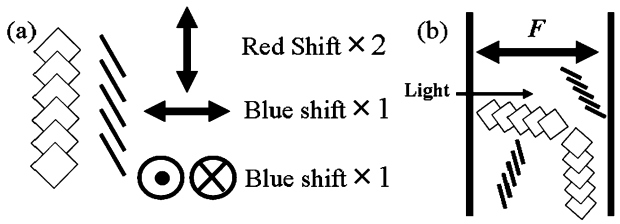

Fig. 4 (a) Six possible directional arrangements of TPPS J-aggregates in aqueous solution. Any arrangement of the aggregates is expressed by the combination of these six arrangements. The broadening effect is dominant when the electric field is applied, because red- and blue-shifts take place evenly. (b) Isotropic orientation of TPPS J-aggregates between ITO glass electrodes.

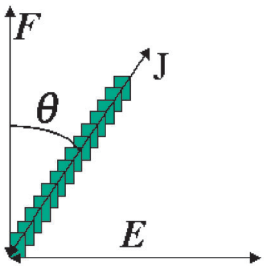

Fig. 5 Model for the aqueous solution, where the applied electric field ***F*** is perpendicular to the optical electric field ***E***. The bonding axis *J* of the TPPS J-aggregate is distributed in between. Actually, ***J*** was distributed three-dimensionally, but it can be reduced to the two-dimensional distribution, as shown here. This is because ***E*** points in all the directions within the plane perpendicular to ***F*** with the use of the unpolarized probe light.

EA spectra of TPPS in aqueous solution

Signal broadening was observed in the EA spectra of the aqueous solution as shown in Fig. 1(b) and (d), which typically reflects the orientation distribution of the static dipole moment. By contrast, the origin of this signal can be attributed to the orientation distribution of the *J*-axis with respect to the applied electric field ***F***, as explained below. In this case, the model predicts that red-, for ***J*** parallel to ***F***, and blue-, for ***J*** perpendicular to ***F***, shifts occur evenly, because there are equivalent contributions of these shifts. This is exactly depicted in Fig. 4(a). More precisely, it is necessary to consider that the applied electric field ***F*** is perpendicular to the optical electric field ***E***, as shown in Fig. 4(b). Fig. 5 shows a model of J-aggregates in an aqueous solution under an applied AC electric field. ***E*** is perpendicular to ***F*** in the experiment; therefore, the components of the applied electric field parallel and perpendicular to the *J*-axis are $F_J = F_0\cos\theta$ and $F_H = F_0\sin\theta$, respectively. The signal magnitude is proportional to $\boldsymbol{F}^2$ and the amount of red-shift is twice as large as that of blue-shift. Therefore, the applied electric field induces red- and blue-shifts as given by the following equations:

$$\int_0^{\pi/2} d\theta\{(F_0\cos\theta)^2 2\sin\theta\} = \frac{2}{3} \quad (5)$$

for red shift, and

$$\int_0^{\pi/2} d\theta\{(F_0\sin\theta)^2\sin\theta\} = \frac{2}{3} \quad (6)$$

for blue shift. Thus, both shifts are expected to have the same size. Therefore, the model is in good agreement with the broadening spectrum, which exhibited both blue- and red-shifts in the J band.

Signal broadening usually reflects the squared absolute value of the difference in the static dipole moment $|\Delta\mu|^2$, which is in the third term of eqn (1).[20] More precisely, it is expressed by

$$|\Delta\mu|^2 = \sum_{i=1}^{n} |\Delta\mu_i|^2/n, \quad (7)$$

where *n* is the number of J-aggregates in the probed region of the sample. This signal could appear when each J-aggregate, *i.e.*, macroaggregate, has a static dipole moment with random orientation. Without symmetry-breaking perturbation, the TPPS J-aggregate has no static dipole moment, because of its centrosymmetry, which originates from the symmetry of the monomer molecule. External perturbation breaks the centrosymmetry, which results in a finite static dipole moment in both excited and ground states. This effect induces broadening of the signal, but perturbation-induced $\Delta\mu$ usually causes much smaller electrooptic signals than intrinsic $\Delta\alpha$, as observed for the film samples in ref. 1. In contrast, ΔA of TPPS in the aqueous solution is unusually large. The signal size in the present condition is approximately 10 000 times larger in $\Delta A/\boldsymbol{F}^2$ than that in a polymer film. This is possibly because constituent monomers in J-aggregates are more readily realigned in liquid water than that in a solid polymer due to the difference in the resonance frequency of molecular rotation.[3] For J-aggregates, the signal strength is given by[2]

$$J \propto -2\frac{kF^2}{(\Omega^2 + 3kF^2)}\theta_0^2\cos 2\omega t, \quad (8)$$

where Ω is the resonance frequency of rotation of the monomer molecule depending on the surroundings, *k* is a constant, θ_0 is the equilibrium angle between the molecular transition dipole moment and the aggregation axis, and ω is the modulation frequency of the applied electric field.

The local field factor, represented by the parameter *s* in eqn (2), is another possible origin for the larger electrooptic signal in aqueous solution than in a polymer film. The static dielectric constant for liquid water is 80, while that for PVA is 5.9, so that the Lorentz local field for the aqueous solution sample is 9 times higher than that for the polymer sample. In eqn (2), s^2 is 81 times larger for the solution than for the polymer film, thus yielding an approximately 100-fold difference. However, there still remains a 100-fold difference.

Contribution of the electric double layer to the large signal in aqueous solution

It is important to consider the contribution of the electric double layer (EDL) to the large electroabsorption signal in aqueous solution as follows. The electrooptic Kerr signal *S* depends on the applied electric field *F* such that

$$S = KF^2, \quad (9)$$

where *K* is the Kerr constant of the sample. If the electric field is uniformly distributed between the electrodes (without EDL),

$$S = kNF^2 = knL(V/L)^2 = knV^2/L, \quad (10)$$

where k is the Kerr constant per molecule, N is the number of molecules, L is the sample thickness, V is the applied voltage, and n is the number density of molecules per thickness ($N = nL$). From eqn (9) and (10),

$$KF^2 = K(V/L)^2 = knV^2/L \quad (11)$$

to obtain

$$K = knL = kN. \quad (12)$$

On the other hand, if the EDL is formed such that the electric field is concentrated on a shorter length of $xL = D$ ($0 < x < 1$, $D = 2d$, d: thickness of EDL) and only the molecules in the EDL respond to the field, then the signal is given by

$$S' = k(nxL)(V/xL)^2 = knV^2/(xL). \quad (13)$$

The Kerr constant of the sample is described by the following relation under the assumption of a uniform electric field given by V/L

$$S' = KF^2 = K(V/L)^2 = knV^2/(xL). \quad (14)$$

As a result, the apparent Kerr constant of the sample is given by

$$K = knL/x = kN/x. \quad (15)$$

The apparent Kerr constant per molecule K/N, which is proportional to $\chi^{(3)}$ per molecule, is given by

$$K/N = k/x = k(L/D). \quad (16)$$

Both are enhanced by a factor of $1/x$ ($=L/D$). This accounts for the large enhancement of the EO signal and $\chi^{(3)}$ for TPPS J-aggregates in aqueous solution compared with those in the polymer film.

Generally, thickness of EDL (d) is given by the Debye length $d = 0.304[\mathrm{Ion}]^{-0.5}$. In the experiment, on the basis of this formula, thickness of the EDL and the number ratio of the molecules present in the EDL *vs.* all the molecules between the electrodes are calculated to be $d = 10$ nm for $[H^+] = 0.001$ mol l^{-1} and the ratio $= 2d/L = 10\ \mathrm{nm} \times 2/0.7 \times 10^{-5}\ \mathrm{nm} = 3 \times 10^{-4}$ without KCl, and $d = 1$ nm for [KCl] = 0.1 mol l^{-1} and the ratio $= 2d/L = 1\ \mathrm{nm} \times 2/0.7 \times 10^{-5}\ \mathrm{nm} = 3 \times 10^{-5}$ with KCl. This estimation of the EDL thickness is consistent with the results in Tables 1 and 2, where $\chi^{(3)}$ is larger with KCl (*i.e.*, thinner EDL) than without KCl.

If the local field correction is neglected, the apparent $\chi^{(3)}$ per molecule for TPPS J-aggregates in aqueous solution is approximately 10 000 times larger than that in the PVA film. In the presence of the EDL, the apparent $\chi^{(3)}$ per molecule in aqueous solution, in Table 1, was estimated to be about L/D (0.35×10^4: without KCl; 0.35×10^5: with KCl) times larger than the true $\chi^{(3)}$. Therefore, the true $\chi^{(3)}$ per molecule in aqueous solution is close to that in a PVA film. However, the size of the EA signal, $\Delta A = 2 \times 10^{-3}$, in Fig. 1b, cannot be explained with $d = 1$ to 10 nm because of the following reason. The peak absorbance of the J-band is about 1, so that the absorbance per unit length is $1/L$. From this, we can estimate the maximum intensity of electroabsorption signal to be D/L (decrease in the absorbance peak) by assuming that complete quenching in absorbance takes place per molecule in the EDL. The maximum value is about 2×10^{-4}, which is ten times smaller than the observed signal $\Delta A = 2 \times 10^{-3}$. This controversy can be explained by considering a thicker EDL, because the formation of the EDL by the AC electric field is presumably not complete. For example, in order to fill in the discrepancy, the EDL thickness has to be thicker than 50 nm at least. In this case, the electric field in the EDL is less than 10^6 V m^{-1} and the true $\chi^{(3)}$ in aqueous solution is more than 10 times larger than that in the polymer film, to which the electric field of more than 3×10^6 V m^{-1} is applied. If the saturation effect of the electroabsorption signal in J-aggregates under the strong electric field in eqn (8) is considered, this discrepancy of $\chi^{(3)}$ is explained by the electric-field dependence of $\chi^{(3)}$ shown in Table 1 of ref. 2.

If the local field correction is taken into account, the apparent $\chi^{(3)}$ per molecule for TPPS J-aggregates in aqueous solution is approximately 100 times as large as that in the PVA film. In the presence of the EDL, the apparent $\chi^{(3)}$ per molecule in aqueous solution, in Table 2, was estimated at about L/D (0.35×10^4: without KCl; 0.35×10^5: with KCl) times larger than the true $\chi^{(3)}$. Therefore, the true $\chi^{(3)}$ per molecule in aqueous solution is about 1/100 times smaller than that in the PVA film. This is again explained by considering the saturation effect of the electroabsorption signal under the strong electric field because the electric field in the EDL is estimated to be enormously large, *i.e.*, 10^9 V m^{-1}, in this experiment. However, the problem of the size of the EA signal remains. This is solved with a thicker EDL as discussed above. If the EDL is thicker than 50 nm, the electric field in the EDL is less than 10^8 V m^{-1} and the true $\chi^{(3)}$ in aqueous solution is 1/10 times or more as large as that in the polymer film. This is also explained by the saturation effect.

In summary, the effects of the EDL are consistent with the experimental observation both with and without the local field correction. Thus the contribution of the EDL is of high possibility.

Electric-field induced long-time response

The long-time spectral response under an electric field is of significant interest. Without KCl, the respective increase and decrease in the intensities of the J- and D-monomer bands are simultaneously observed, as shown in Fig. 2a. These changes are considered to correspond to the progress in aggregation associated with the applied electric field. One possible mechanism for the enhancement of aggregation is the electric-field induced alignment of monomer molecules. The diacid TPPS molecule is a disk-like molecule with D_{4h} symmetry, so that the dipole moment is induced in the molecular plane by the electric field and it is oriented in the direction of the electric field. This results in alignment of the molecular planes of the D-monomer molecules parallel to the electric field. When such monomers encounter each other, aggregates are formed with higher probability than monomers of random orientation.

In contrast, Fig. 2b shows dissociation of J-aggregates in the solution with KCl under an electric field. From eqn (4), the blue (red)-shift of the absorption peak of J-(H-)aggregates indicates reduction in the coherent aggregation number N.

The increase in the height of the F-monomer band indicates an increase in the number of F-monomer molecules. The peak energies of the coherent aggregates for dimers ($N = 2$), trimers ($N = 3$) and tetramers ($N = 4$) are estimated to be 460, 472 and 478 nm, respectively, according to eqn (4) with $k = 1$, which corresponds to the lowest-energy dipole-allowed exciton state in the J-aggregate with the largest red-shift from the D-monomer peak. The spectra in Fig. 2c strongly suggest that coherent aggregates of such a small number of N were formed in the course of dissociation, although it is not clear whether N-mers are isolated from one another or constitute macroaggregates.

One of the possible dissociation mechanisms in J-aggregates is the involvement of K^+ ions, which neutralize excess charges in D-monomers to promote the formation of J-aggregates. If the electric field causes detachment of K^+ ions from the constituent D-monomers, the J-aggregates are split into fragments under the electric field. For this mechanism to take place requires that K^+ ions be more loosely bound in the D-monomer than H^+. This is because aggregation in the solution without KCl was found to be promoted by the electric field, where H^+ plays a major role in neutralization instead of K^+.

It is noteworthy that the D-monomer band did not appear during this dissociation process. Considering that J-aggregates are composed of D-monomers, it is expected that the D-monomer band should appear before the F-monomer band is substantially increased by dissociation.

It appears that there was an isosbestic point at 456 nm in the long-time response for the TPPS solution without KCl in Fig. 2a. If this point exists, then the absorbance changes are not induced by the change in the coherent size of the J-aggregates, but by the change in the concentration ratio between the two species, the F-monomer and the J-aggregate of certain size. However, when the magnified spectra are closely examined, as shown in Fig. 2d, the initial spectrum (black) intersects the other spectra (colored) and the colored spectra have an isosbestic point at 456.7 nm. This indicates that the coherent size was initially increased, but was immediately saturated (from black to colored spectra). The concentration of J-aggregates of a certain saturated size (sufficiently large N) then increased against that of the F-monomer. In contrast, no isosbestic point was observed for the solution with KCl, which demonstrates that the coherent size of the J-aggregates was gradually varied by dissociation into a smaller size.

There have been reports that the coherent length of aggregates is controlled by a change in the experimental parameters,[38–41] where the aggregation number N is evaluated from a small energy shift or change in the bandwidth of the absorption spectra. There is no example where such a large absorption change is observed, as shown in Fig. 2, by simply applying an electric field.

Effects of redox potential

We have to consider the effect of the electrochemical oxidation and reduction processes on the change in the aggregation number of TPPS.

When the electric field was applied, TPPS J-aggregates in aqueous solution with KCl showed blue shift of the J-band, which indicates the dissociation of the J-aggregates, while those without KCl showed the increase in the absorbance of the J-band. These results do not depend on whether the applied fields are DC or AC fields, but only depend on whether KCl is added or not. This is a negative fact against the possible contribution of the electrochemical redox reactions.

In addition, redox potentials of TPPS molecules were reported to be as midpoint potentials 1.10 V for oxidation and −1.06 V for reduction *vs.* NHE (normal hydrogen electrode).[42,43] Since we did not use a standard reference electrode, we do not know to what value of potential TPPS molecules are precisely exposed. But the fact that dissociation of J-aggregates took place even when the applied AC electric field was as small as 0.1 V p–p (Fig. 1b and 3b, d and f). This is against the possible contribution of the electrochemical redox reactions.

On the other hand, there was recognizable difference in absorption spectra between the F-monomer and the final decomposed products which appeared around 400–420 nm at the end of the dissociation. The absorption spectrum of the F-monomer does not completely accord with the dissociation spectra. In addition, there were red-shifted components in the spectra of the dissociated systems as in Fig. 2b and c and once the system was dissociated, they were hardly reassembled to form J-aggregates again even after the electric field was off. These facts suggest the possibility of some irreproducible electrochemical reactions taking place in TPPS molecules.

To conclude, the electrochemical redox reactions are not a main mechanism of the change in the aggregation states of J-aggregates by the electric field, but there are some unexplained experimental results which cannot completely reject contributions of electrochemical reactions.

Equilibrium conditions of J-aggregate formation

There is a large difference in the long-time response between the two samples with and without KCl. This should reflect the role of KCl in the aggregation mechanism. A sufficient concentration of H^+ (proton), *i.e.*, sufficient TTPS concentration, because it ionizes into $F^{4-} + 4H^+$, results in di-protonation of the F-monomer (H_2TPPS^{4-}) into the D-monomer (H_4TPPS^{2-}). For the J-aggregate to be formed, two more cations are required for neutralization. With a sufficiently high concentration of K^+, the J-aggregates are probably comprised of D-monomers and K^+ ions are donated by KCl, instead of protons.

The mechanism for the formation of TPPS J-aggregates without KCl is described in terms of the equilibrium among protons, F-monomers, D-monomers and J-aggregates. The supplied concentration of TPPS molecules [TPPS] and that of protons [H_{all}], which are ionized from TPPS molecules, satisfy the following equations:

$$[\mathrm{TPPS}] = [\mathrm{F}] + [\mathrm{D}] + 2[\mathrm{J}_2] + 3[\mathrm{J}_3] + \cdots + n[\mathrm{J}_n], \quad (17)$$

$$[\mathrm{H}_{all}] = [\mathrm{H}] + 2[\mathrm{D}] + 8[\mathrm{J}_2] + 12[\mathrm{J}_3] + \cdots + 4n[\mathrm{J}_n], \quad (18)$$

where [F], [D], [J_i] and [H] are the concentrations of the F-monomer, D-monomer, J-aggregates with aggregation number i, and protons, respectively. When TPPS molecules are entirely ionized, *i.e.*, TPPS → $F^{4-} + 4H^+$, the equilibrium

between [H], [F], [D], [J_2] (dimer), [J_{i-1}], and [J_i] is given by the following relations:[44]

$$[F][H]^2 = k_d[D]$$

$$[D]^2[H]^4 = k_2[J_2]$$

$$[J_{i-1}][D][H]^2 = k_i[J_i], \quad (19)$$

where k_d and k_i are equilibrium constants for the relevant reaction.

The reaction between J-aggregates and monomer molecules is usually assumed to be N[M] = [J], as previously reported.[45–47] That is, J-aggregates are considered to be a single species with a fixed aggregation number N. In the present experiment, however, the aggregation number N takes various values, as shown in Fig. 2, so that eqn (19) is a more appropriate representation than an expression such as N[M] = [J].

Eqn (20) and (21) can be obtained from eqn (17) and (18) with eqn (19) by assuming $k_2 = k_3 = \cdots = k_n = k$.

$$[TPPS] = \frac{k_d[D]}{[H]^2} + [D] + \frac{2}{k}[H]^4[D]^2 + \frac{3}{k^2}[H]^6[D]^3 + \cdots + \frac{n}{k^{n-1}}[H]^{2n}[D]^n \quad (20)$$

$$[H_{all}] = [H] + 2[D] + \frac{8}{k}[H]^4[D]^2 + \frac{12}{k^2}[H]^6[D]^3 + \cdots + \frac{4n}{k^{n-1}}[H]^{2n}[D]^n \quad (21)$$

With no other cations than protons, [H_{all}] is equivalent to 4[TPPS], because the F-monomer is a tetravalent anion. Therefore, the concentration of the D-monomer is expressed by [H] as

$$[D] = \frac{[H]}{2}\left(2k_d\frac{1}{[H]^2} + 1\right)^{-1} \quad (22)$$

The concentrations of the F- and D-monomers and J-aggregates can then be estimated from eqn (19), (20) and (22), if the supplied concentration of TPPS molecules, [*TPPS*], k_d and k are given.

The concentrations of F-, D-monomers and J-aggregates estimated from eqn (19), (20) and (22) with $k_d = 2 \times 10^{-6}$ and $k = 1.5 \times 10^{-9}$ are listed in Table 3 with $n = 20$ as the largest

Table 3 Calculated concentrations of F-monomer, D-monomer, and J-aggregates in the solution without KCl, from eqn (12) and (14). The TPPS concentrations in the experiments in Fig. 1–3 are close to 8.1×10^{-4} mol l^{-1}

[TPPS]/mol l^{-1}	[F] (%)	[D] (%)	[J($16 \le N \le 20$)] (%)
1×10^{-5}	99.9	0.079	0
2.5×10^{-5}	99.5	0.49	0
1×10^{-4}	92	7.4	0
3×10^{-4}	67	33	0
8.1×10^{-4}	31	62	6
0.0011	24	50	23
0.012	2.2	5.0	89
0.12	0.22	0.53	97

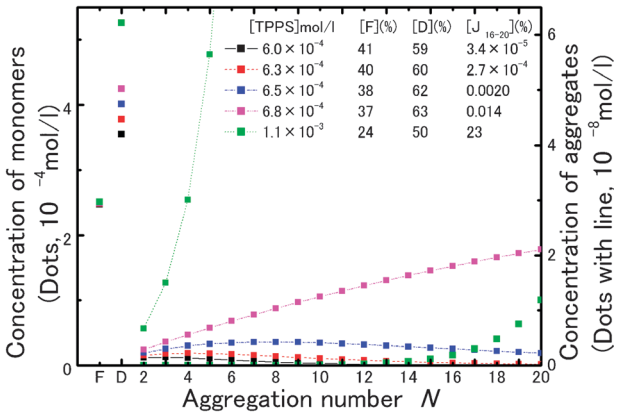

Fig. 6 Concentration of monomers and aggregates with various aggregation numbers, as calculated from eqn (19), (20) and (22). For the calculation, the proton concentration is assumed to derive the concentrations of the other species. When the concentration ratio of monomers (F + D) to aggregates (J_{2-20}) is 99.9 : 0.1, J-aggregates with $N \ge 16$ are already dominant in concentration over those with $N < 15$. This explains why experimentally observed aggregates are always well-grown aggregates with a large aggregation number N.

aggregation number for a coherent aggregate. k_d was estimated from eqn (19) with [TPPS] = 3.5×10^{-5} mol l^{-1} and [D] ≪ [F]. Table 3 explains why only those J-aggregates that are substantially red-shifted are observed for any concentration. Well-grown aggregates with $n > 15$ occupy most of the concentration of the aggregates if [TPPS] > 0.0012 mol l^{-1}. The calculated results given in Table 3 and Fig. 6 reproduce the features of the TPPS aqueous solution absorption spectra very well.

With KCl, K^+ ions in addition to H^+ serve to neutralize excess charge in the D-monomer for the formation of J-aggregates. Fig. 7 shows the absorption spectra of TPPS as a function of the KCl concentration. For TPPS of 3×10^{-4} mol l^{-1} with a low concentration of KCl, the absorption spectrum shows two peaks characteristic of the F and D monomers at 412 and 433 nm, respectively. With increasing KCl, the J-bands at 490 and 707 nm increase while the monomer bands decrease. Finally the D-monomer band is completely

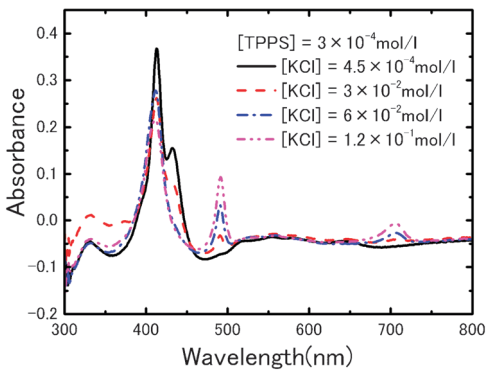

Fig. 7 Absorption spectra of TPPS in aqueous solutions with different concentrations of KCl. Black (solid), red (dashed), blue (dash-dotted) and magenta (dash-dot-dotted) lines show absorption spectra with the KCl concentrations of 4.5×10^{-4}, 3×10^{-2}, 6×10^{-2} and 1.2×10^{-1} mol l^{-1}, respectively.

quenched while the F-monomer band has a significant magnitude.

In this situation, eqn (19) can be rewritten with [K] as eqn (23).

$$[F][H]^2 = k_d[D]$$

$$[D]^2([H] + c[K])^4 = k_2[J_2],$$

$$[J_{i-1}][D]([H] + c[K])^2 = k_i[J_i] \quad (23)$$

where c is a parameter to introduce the difference in the equilibrium constants between K^+ and H^+. $[H_{all}]$ and the supplied concentration of K^+ ions $[K_{all}]$ satisfy the following equations:

$$[H_{all}] = [H] + 2[D] + \frac{2[H] + c[K]}{[H] + c[K]}(4[J_2] + 6[J_3] + \cdots + 2n[J_n]) \quad (24)$$

$$[K_{all}] = [K] + \frac{c[K]}{[H] + c[K]}(4[J_2] + 6[J_3] + \cdots + 2n[J_n]) \quad (25)$$

The concentration of the D-monomer is given by

$$[D] = \frac{[H] + [K] - [K_{all}]}{4\frac{k_d}{[H]^2} + 2} \quad (26)$$

and eqn (17) is revised to

$$[TPPS] = \frac{k_d[D]}{[H]^2} + [D] + \frac{2}{k}([H] + c[K])^4[D]^2 + \frac{3}{k^2}([H] + c[K])^6[D]^3 + \cdots + \frac{n}{k^{n-1}}([H] + c[K])^{2n}[D]^n \quad (27)$$

The concentrations of the F-, D-monomers and J-aggregates can then be estimated using eqn (23), (26) and (27), if [H] is given, as listed in Table 4. The experimental spectral features of TPPS in aqueous solution with KCl shown in Fig. 7 are reproduced fairly well by the calculation with $c = 0.12$. Note that [D] decreases more rapidly than [F] with [Kall]. For $c < 1$, the K^+ ions play a less important role in the formation of J-aggregates than H^+. In other words, K^+ ions are more loosely bound in the D-monomer than H^+, which is consistent with the dissociation mechanism under an electric field as considered in Fig. 1(b) and (c).

In the present analyses, the complexity of the equilibrium between macroaggregates and microaggregates is omitted, because the absorption spectra of J-aggregates are mainly characterized by microaggregates rather than macroaggregates.

Table 4 Calculated concentrations of F-monomer, D-monomer, and J-aggregates for the solution with KCl, from eqn (15), (18) and (19). The KCl concentration used in the experiments in Fig. 1–3 is 0.1 mol l^{-1}

$[K_{all}]$/mol l^{-1}	[TPPS]/mol l^{-1}	[F] (%)	[D] (%)	[J($16 \leq N \leq 20$)] (%)
0.00045	0.0003	67	33	0
0.03	0.0003	65	30	4
0.06	0.0003	37	11	46
0.12	0.0003	15	3	74

The present analyses are appropriate as long as microaggregates are not spectrally discriminated from macroaggregates. In the next section, we distinguish microaggregates from macroaggregates on the basis of the EM spectra of them. In this case, more parameters are required to explain the equilibrium between micro and macroaggregates.[44,45]

We can argue about the effect of the EDL on the dissociation and the association processes of J-aggregates in solution. The formation of a more compact EDL and the resulting strong electric field with the addition of K^+ ions reinforce dissociation of J-aggregates in addition to the fact that K^+ ions are more loosely bound in the D-monomer than H^+. Therefore, the contribution of the EDL further supports our proposed dissociation mechanism with KCl. Without KCl, the EDL is thicker and thus the electric field is weaker than with KCl, so that H^+ ions, which are more tightly bound than K^+ ions, are hard to be removed. Yet the enhancement of the aggregation probability due to the electric-field induced alignment of the molecular planes is still effective even with the EDL involved. Thus, the contribution of the EDL is consistent with our proposed mechanisms of both dissociation and association processes.

Electromodulation spectra of the coherent aggregates

The absorbance changes induced by application of an electric field for 2 h were accompanied by changes in the EM spectra. The electrooptic parameters for the samples without KCl showed little change over 75 min, because the peak energy of the J band was invariant, as shown in Fig. 3a, c and e. In contrast, the samples with KCl had significant changes in the EM spectra, as shown in Fig. 3b, d and f.

The coherent aggregation number N can be estimated from the J-band peak energy. For $N \gg 10$, the broadening component dominates over the shift component, similar to the signal observed for the solution without KCl. However, for $N = 10$, the shift component becomes as large as the broadening one. For $N < 10$, the shift component dominates over the broadening component, as shown in Fig. 3f.

For isotropic distribution of macro-J-aggregates in aqueous solution, the broadening signal is expected according to the rearrangement model. However, the situation should be different for microaggregates. F-monomers were finally formed by application of the stationary electric field with KCl, as shown in Fig. 2b and c; therefore, it is reasonable to assume that the spectrally observed N-mers do not constitute macroaggregates, but are microaggregates dissociated from macroaggregates. If this is the case, then the coherent aggregates would be readily oriented along the direction of the electric-field, since the size of the coherent aggregates is much smaller than that of the macroaggregates considering the following reason.

The torque τ of dipole moments induced by the applied electric field for the J-aggregates is given by

$$\tau = (\text{Force}) \times a = I\frac{d\omega}{dt}, \quad (28)$$

where a is the length of the J-aggregates, I is the moment of inertia of the macro or microaggregates, and ω is the angular velocity of the induced dipole moments. For a rod-like

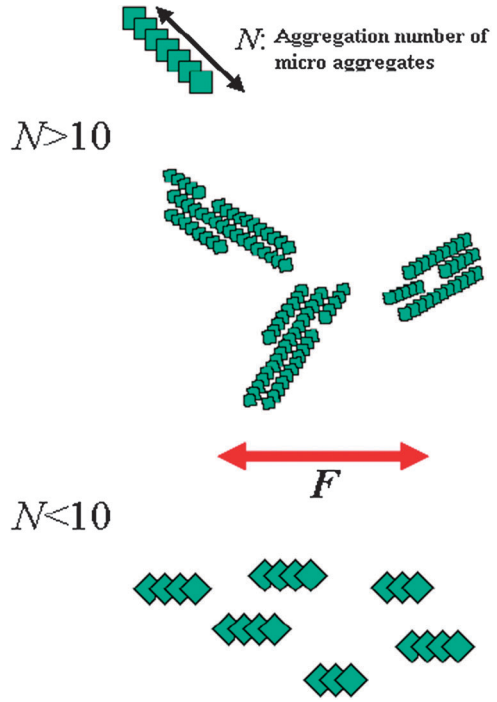

Fig. 8 Response of the TPPS macro and microaggregates to the applied electric field ***F***. The TPPS macro-J-aggregates are made up of a lot of microaggregates, so that they are hard to be rotated by the electric-field-induced torque because of the large moment of inertia. Microaggregates, on the other hand, are readily rotated by the electric field to be aligned in the direction of the electric field, resulting in a quasi-one-dimensional distribution.

structure, the moment of inertia I is proportional to a^2. The angular acceleration can then expressed by

$$\frac{d\omega}{dt} \propto \frac{1}{a}. \qquad (29)$$

Eqn (29) shows that the angular acceleration is larger for microaggregates than for macroaggregates, *i.e.*, microaggregates can be readily aligned by the electric field. In the case of quasi-one-dimensional orientation of J-aggregates along the direction of the applied electric field, the rearrangement model predicts a red-shift of the J band, as depicted by Fig. 6 in ref. 2.

Therefore, we conclude that the changes in the EA spectra with decreasing aggregation number are explained by the rearrangement model and by the difference between macro and microaggregates, as shown in Fig. 8. When N is sufficiently large ($N \gg 10$), the broadening signal predominates in the EM spectra. This is explained by immobile macroaggregates with $N \gg 10$. When N is sufficiently small ($N < 10$), then the red-shift signal predominates in the EM spectra. This is explained by mobile, rotatable microaggregates with $N < 10$. We conclude that macroaggregates break into microaggregates with diminution of N under a stationary electric field.

Conclusion

New evidence was found that indicates the molecular rearrangement model is an appropriate model to explain the large enhancement of $\Delta\alpha$ due to the formation of TPPS J-aggregates. A large broadening signal was measured in the aqueous solution, and the $\chi^{(3)}$ in the aqueous solution was 10^4 times larger than that in the polymer film. These results are reasonably explained by the rearrangement model. The much larger $\chi^{(3)}$ in the aqueous solution than in the polymer film can be explained by considering the contribution of the electric double layer formed at the interface between the electrode and the solution.

The dissociation and aggregation processes of J-aggregates in solutions with and without KCl, respectively, were observed as the long-term change in the absorption spectra with application of an electric field over 2 h. Without KCl, the concentration of well-grown aggregates with a large coherent size increased with time. With KCl, the absorption and EM spectra strongly suggest that macroaggregates composed of microaggregates with a large coherent size are dissociated into microaggregates with small coherent size over time. The large difference in the long-time response between the samples with and without KCl reflects the role of K^+ ions in the aggregation mechanism. The equilibrium constants for aggregate formation from monomers were derived and were shown to reproduce the concentration dependence of the absorption spectra. K^+ was found to be more loosely bound to the constituent monomers in J-aggregates than H^+, which is in agreement with the observed dissociation behavior under an electric field. These results provide clues to establish a method for the fabrication of microaggregates with a desired coherent aggregation number N. If this is realized, a spectroscopic study of single coherent aggregates would reveal the detailed structure of optically excited states in J-aggregates beyond the simplest Frenkel exciton model.[48]

Acknowledgements

This work was supported by the Core Research for Evolutional Science and Technology (CREST) program of the Japan Science and Technology Agency (JST), the National Science Council of the Republic of China, Taiwan (NSC 98-2112-M-009-001-MY3), and a grant from the Ministry of Education, Aiming for Top University (MOE ATU) Program at National Chiao-Tung University (NCTU). A part of this work was performed under the joint research project of the Institute of Laser Engineering, Osaka University under Contract No. A3-01.

References

1 T. Ogawa, E. Tokunaga and T. Kobayashi, *Chem. Phys. Lett.*, 2005, **408**, 186.
2 T. Katsumata, K. Nakata, T. Ogawa, K. Koike, T. Kobayashi and E. Tokunaga, *Chem. Phys. Lett.*, 2009, **477**, 150.
3 K. Nakata, T. Kobayashi and E. Tokunaga, *Opt. Rev.*, 2010, **17**, 346.
4 K. Misawa and T. Kobayashi, *Nonlinear Opt.*, 1995, **14**, 103.
5 H. Wendt and J. Friedrich, *Chem. Phys.*, 1996, **210**, 101.
6 T. Kobayashi, *Mol. Cryst. Liq. Cryst.*, 1998, **314**, 1.
7 O. Ohno, Y. Kaizu and H. Kobayashi, *J. Chem. Phys.*, 1993, **99**, 4218.
8 N. C. Maiti, S. Mazumder and N. Periasamy, *J. Phys. Chem.*, 1995, **99**, 10708.

9 N. C. Maiti, S. Mazumder and N. Periasamy, *J. Phys. Chem.*, 1998, **102**, 1528.
10 T. Kobayashi, T. Saito, C. Hikage and K. Misawa, *Meet. Abstr. Phys. Soc. Jpn.*, 1998, **53**, 221.
11 K. Misawa and T. Kobayashi, *Technical Digest of IQEC'98*, 1998, p. 99.
12 A. Eilmes, *Chem. Phys. Lett.*, 2001, **347**, 205.
13 Y. Kitahama, Y. Kimura and K. Takazawa, *Langmuir*, 2006, **22**, 7600.
14 D. A. Higgins and P. F. Barbara, *J. Phys. Chem.*, 1995, **99**, 3–7.
15 P. J. Reid, D. A. Higgins and P. F. Barbara, *J. Phys. Chem.*, 1996, **100**, 3892–3899.
16 D. A. Higgins, P. J. Reid and P. F. Barbara, *J. Phys. Chem.*, 1996, **100**, 1174–1180.
17 H. von Berlepsch, C. Böttcher and L. Dähne, *J. Phys. Chem. B*, 2000, **104**, 8792.
18 R. Rotomskis, R. Augulis, V. Snitka, R. Valiokas and B. Liedberg, *J. Phys. Chem. B*, 2004, **108**, 2833.
19 D. M. Chen, T. He, D. F. Cong, Y. H. Zhang and F. C. Liu, *J. Phys. Chem. A*, 2001, **105**, 3981.
20 W. Liptay, in *Excited States*, ed. E. C. Lim, Academic Press, New York, 1974, p. 129.
21 A. Chowdhury, S. Wachsmann-Hogiu, P. R. Bangal, I. Raheem and L. A. Peteanu, *J. Phys. Chem. B*, 2001, **105**, 12196.
22 K. Misawa, K. Minoshima, H. Ono and T. Kobayashi, *Chem. Phys. Lett.*, 1994, **220**, 251.
23 D. S. Gottfried and S. G. Boxer, *J. Lumin.*, 1992, **51**, 39.
24 K. Nakagawa, S. Suzuki, R. Fujii, A. T. Gardiner, R. J. Cogdell, M. Nango and H. Hashimoto, *J. Phys. Chem. B*, 2008, **112**, 9467–9475.
25 K. Yanagi, A. T. Gardiner, R. J. Cogdell and H. Hashimoto, *Phys. Rev. B: Condens. Matter*, 2005, **71**, 195118.
26 K. Yanagi, M. Shimizu, H. Hashimoto, A. T. Gardiner, A. W. Roszak and R. J. Cogdell, *J. Phys. Chem. B*, 2005, **109**, 992–998.
27 K. Yanagi, H. Hashimoto, A. T. Gardiner and R. J. Cogdell, *J. Phys. Chem. B*, 2004, **108**, 10334–10339.
28 H. Kishida, Y. Nagasawa, S. Imamura and A. Nakamura, *Phys. Rev. Lett.*, 2008, **100**, 097401.
29 H. Kishida, K. Hirota, T. Wakabayashi, B. Lee, H. Kokubo, T. Yamamoto and H. Okamoto, *Phys. Rev. B: Condens. Matter*, 2004, **70**, 115205.
30 J. Tayama, T. Iimori and N. Ohta, *J. Chem. Phys.*, 2009, **131**, 244509.
31 R. Mathies and L. Stryer, *Proc. Natl. Acad. Sci. U. S. A.*, 1976, **73**, 2169.
32 H. Hiramatsu and H. Hamaguchi, *Appl. Spectrosc.*, 2004, **58**, 355.
33 M. Khoudiakov, A. R. Parise and B. S. Brunschwig, *J. Am. Chem. Soc.*, 2003, **125**, 4637.
34 Y. K. Shin, B. S. Brunschwig, C. Creutz and N. Sutin, *J. Phys. Chem.*, 1996, **100**, 8157.
35 N. Ishii, E. Tokunaga, S. Adachi, T. Kimura, H. Matsuda and T. Kobayashi, *Phys. Rev. A*, 2004, **70**, 023811.
36 R. Worland, S. D. Phillips, W. C. Walker and A. J. Heeger, *Synth. Met.*, 1989, **28**, D663.
37 T. Kobayashi, *J-Aggregates*, World Scientific, Singapore, 1996.
38 A. S. R. Koti, J. Taneja and N. Periasamy, *Chem. Phys. Lett.*, 2003, **375**, 171.
39 U. De Rossi and S. Daehne, *Langmuir*, 1996, **12**, 1159.
40 A. Chowdhury, L. Yu, I. Raheem, L. Peteanu, L. A. Liu and D. J. Yaron, *J. Phys. Chem. A*, 2003, **107**, 3351.
41 O. Karthaus and Y. Kawatani, *Jpn. J. Appl. Phys.*, 2003, **42**, 127.
42 R. H. Schmehl and D. G. Whitten, *J. Phys. Chem.*, 1981, **85**, 3473.
43 K. Kalyanasundaram and M. Neumann-Spallart, *J. Phys. Chem.*, 1982, **86**, 5163.
44 F. Oosawa and M. Kasai, *J. Mol. Biol.*, 1962, **4**, 10.
45 R. F. Pasternack, J. I. Goldsmith, S. Szep and E. J. Gibbs, *Biophys. J.*, 1998, **75**, 1024.
46 H. Nagatani and H. Watarai, *Anal. Chem.*, 1998, **70**, 2860.
47 A. S. Tatikolov and S. M. B. Costa, *Chem. Phys. Lett.*, 2001, **346**, 233.
48 R. Schuster, M. Knupfer and H. Berger, *Phys. Rev. Lett.*, 2007, **98**, 037402.